Lunar Gravitational Field as Determined from Lunar Orbiter Tracking Data

JOHN P. GAPCYNSKI,* W. THOMAS BLACKSHEAR,* AND HAROLD R. COMPTON*
NASA Langley Research Center, Langley Station, Hampton, Va.

This paper presents results that have recently been obtained at the NASA Langley Research Center on the problem of determining the gravitational field of the moon from an analysis of the tracking data from the United States Lunar Orbiter series of spacecraft. A set of coefficients defining the gravitational field through degree and order 7 are presented. The results were obtained by a procedure involving combined solutions for a number of well-distributed and relatively short data arcs from the various missions. Although the results represent a considerable improvement over previous solutions, the residual characteristics indicate that higher degree and order terms must be considered in future analyses.

Nomenclature

a = assumed mean radius of the moon, 1738.09 km
C_{nm}, S_{nm} = coefficients in the spherical harmonic expansion of the lunar gravitational potential function
GM = product of the lunar mass and the gravitational constant, 4902.58 km³/sec²
P_{nm} = associated Legendre polynomials of degree n and order m
r = selenographic radius
r_p = satellite periapse radius
U = external lunar gravitational potential function
λ = selenographic longitude
ϕ = selenographic latitude

Introduction

SINCE the first of the Lunar Orbiter series of missions in August of 1966, five United States spacecraft have been successfully placed in orbit around the moon. The primary mission of each of the flights was to obtain high-resolution photographs of specific areas on the lunar surface. A secondary objective of this series of missions was the utilization of the tracking data to define the gravitational field of the moon. In this respect, the determination of the lunar gravitational field has been subject to a continuing analysis as data from each mission were received, and the results of a portion of this work have been reported in Refs. 1–8.

During the course of these analyses, it has become increasingly evident that the adequate definition of the lunar gravitational field requires the inclusion of the higher degree and order harmonics in the solution. Because of the restrictive nature of the available data, however, this requirement introduces the problem of high correlations between certain gravity coefficients, leading to biased estimates of these parameters and correspondingly weak solutions. The technique of using relatively short data arcs for the solution has been found to partially alleviate this problem. It is the purpose of this paper to present the results which have recently been obtained with the use of this technique, and also to discuss the limitations associated with these results and indicate the direction in which future work in this area must proceed.

Method of Analysis

The definition of the lunar gravitational field involves the determination of a finite number of coefficients, C_{nm} and S_{nm}, in the spherical harmonic expansion of the external lunar gravitational potential function in the form given in Eq. (1)

$$U = \frac{GM}{r}\left[1 + \sum_{n=2}^{\infty}\sum_{m=0}^{n}\left(\frac{a}{r}\right)^n P_{nm}(\sin\phi) \times (C_{nm}\cos m\lambda + S_{nm}\sin m\lambda)\right] \quad (1)$$

At the NASA Langley Research Center (LRC), the primary method used for the determination of the gravity coefficients is an approach based on the minimization of the weighted sum of squares of the observational residuals, and utilization of differential corrections to obtain successive improvements in the values of the parameters. The partial derivatives required in the estimation process are the partial derivatives of the observable with respect to the parameters being estimated. The equations of motion and the variational equations are integrated numerically in the Cowell form using a 12th-order predictor-corrector technique.

The results obtained prior to those presented in this paper are given in Ref. 1, and include solutions for coefficients through degree and order 5. The results were obtained from an analysis of the tracking data from the 1st, 3rd, and 4th Lunar Orbiter missions, utilizing long data arcs of from 14 to 21 day's duration. Although the results appeared to give reasonably good predictions of orbital variations over periods of time beyond those for which the data were analyzed, application of these results to the data from the 5th mission and to the nearly circular orbital phase of the third mission proved to be extremely disappointing. In addition, large correlations existed between certain pairs of coefficients (e.g., correlations of 0.87 between C_{20} and C_{40}, and 0.93 between C_{30} and C_{50}). The residual characteristics from this solution also indicated that higher degree and order coefficients should be included in the solution and therefore an attempt was made to increase the size of the solution set to include all coefficients through degree and order 7. This was not feasible, however, because of the large correlations which existed between the higher- and lower-degree terms.

In the analysis of this problem, it was determined that these difficulties could be circumvented, to a large degree, if utilization was made of relatively short data arcs, the epochs of each arc being chosen on the basis of obtaining an even distribution of periapse positions on the lunar surface within the limitations of the orbital geometries available. Several advantages were immediately apparent with the utilization of this technique. With the proper selection of data arcs, the correlations between coefficients could be reduced. Thus, the number of coefficients included in the solution

Presented as AAS Paper 68-132 at the AAS/AIAA Astrodynamics Specialist Conference, Jackson, Wyo., September 3–5, 1968; submitted December 4, 1968; revision received March 19, 1969.

* Aerospace Technologists.

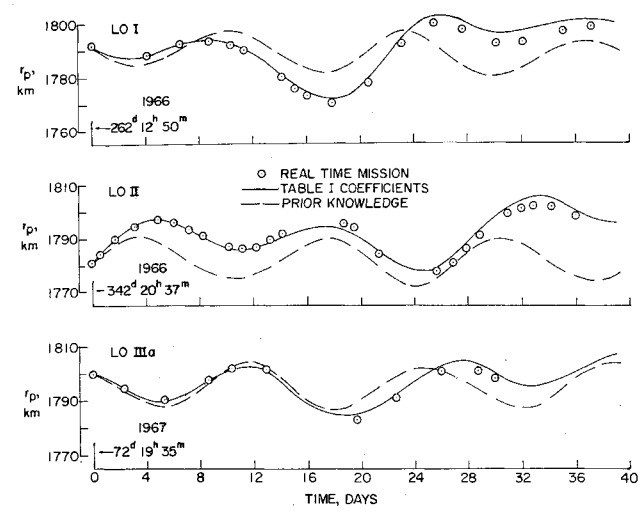

a) Lunar Orbiters I, II, and IIIa

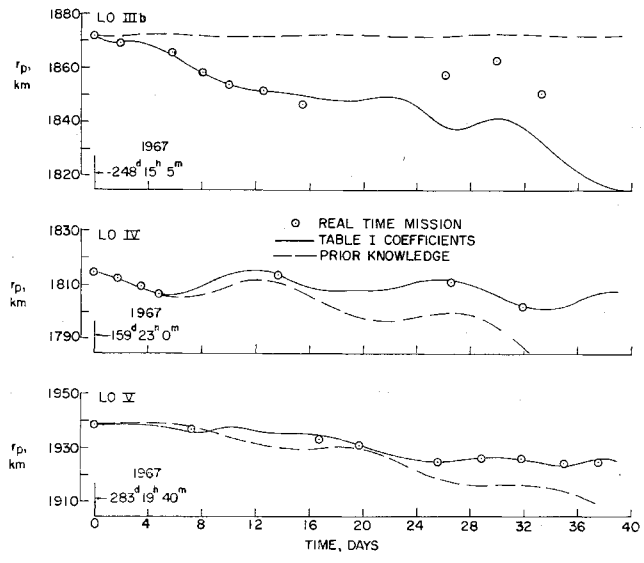

b) Lunar Orbiters IIIb, IV, and V

Fig. 1 Variation of satellite periapse radius with time.

could be increased and the stability of the solution maintained. In addition, the flexibility in the selection of data from the various missions was increased and the over-all computer time substantially reduced.

Orbital Geometry and Tracking Data Arcs

The orbital characteristics for each satellite and a summary of the data included in the solution are presented in Table 1. The first three missions were designed specifically to provide photographic coverage of proposed Apollo landing sites, and therefore the orbital characteristics in each case were similar. In particular, the orbital inclinations were restricted to relatively low values (less than 22°). The orbital characteristics for the 3rd mission were changed so as to provide for a configuration with a small value of eccentricity. This particular configuration has provided some of the more interesting results with regard to the character of the observational residuals during the analysis. The 4th and 5th missions were general photographic mapping missions with orbital inclinations of approximately 85°. In all cases, the satellite periapse location was restricted to regions near the lunar equator. It is to be noted that this combination of restricted orbital inclination and periapse location is not optimal for the purposes of selenodesy.

The results presented in this paper utilized data from all of the orbital configurations. A total of 21 arcs of data, distributed as shown in Table 1, were included in the solution. The length of the data arcs ranged from approximately 1–5 days.

Results on the Lunar Gravitational Field

The values of the lunar gravity field coefficients obtained in this analysis are presented in Table 2. All coefficients through degree and order 7 were included in the solution. In general, although the correlations between the various coefficients were reduced significantly from those obtained in previous solutions, some of the values are still considered to be quite high (e.g., a value of 0.62 between C_{20} and C_{40}, 0.41 between C_{30} and C_{50}, and 0.71 between C_{50} and C_{70}).

No coefficient comparison is made here between these results and the results obtained previously at LRC and other research centers. It is difficult to establish a comparison on a coefficient basis because of the high correlations existing between coefficients in each case and the variations that occur in the size of the various solution sets. Also, published results to date, in general, have proved to be disappointing when utilized to predict satellite states over periods of time which extended beyond the data arcs used in the analysis.

As one measure of the quality of the results presented in Table 2, the prediction of the variations of satellite periapse radius with time, for a period of 40 days, are presented in Fig. 1 for all 6 orbital configurations. The results are compared with values obtained from the determination of the satellite states by The Boeing Company for real-time mission control. In addition, the pericenter variations are presented for a field consisting of those coefficients (nominal values) which had been estimated prior to the Lunar Orbiter flights, that is, $C_{20} = -2.0 \times 10^{-4}$ and $C_{22} = 0.2 \times 10^{-4}$.

The comparison for Lunar Orbiters IV and V (high-inclination orbits) is excellent, and for Lunar Orbiters I, II, and IIIa the agreement is reasonably good. For the low-eccentricity orbit of Lunar Orbiter III, however, the agreement is disappointing. It is possible that the comparison could be improved considerably with the utilization of additional data from this particular configuration. However, the indications are that this particular satellite is strongly influenced by higher-order gravity coefficients and therefore additional analyses should be aimed at including such terms.

Since the application of the results of a given set of gravity coefficients to the low-eccentricity orbit of Lunar Orbiter III is of prime importance for the Apollo mission, an additional test of the results given in Table 2 was made for this orbit configuration. Using tracking data that had not been included in the coefficient determination process, a solution for the satellite state was obtained from an analysis of about 10 hr of data. With this satellite state, the data arc was then extended to about 20 hr. The residuals at this time are shown in Fig. 2. The results from the preknowledge field and the degree and order 5 field of Ref. 1 are included for comparison purposes. It is evident from the results that

Table 1 Orbital geometry and tracking data

Lunar Orbiter	I	II	IIIa	IIIb	IV	V
Semimajor axis, km	2670	2702	2688	1968	3751	2832
Eccentricity	0.327	0.341	0.332	0.062	0.516	0.317
Inclination, deg[a]	12	18	21	21	84	85
Period, min	206	210	208	130	344	225
Data arcs used	2	2	4	3	4	6
Observations used	908	934	3871	1334	4730	3352

[a] Inclination to lunar equator.

Table 2 Lunar gravitational coefficients

n	m	C_{nm}	S_{nm}
2	0	-2.192×10^{-4}	...
	1	-0.9019×10^{-5}	-0.5564×10^{-5}
	2	0.3293×10^{-4}	-0.3910×10^{-5}
3	0	-0.1953×10^{-4}	...
	1	0.2718×10^{-4}	0.4071×10^{-5}
	2	0.6932×10^{-5}	0.4413×10^{-5}
	3	0.2583×10^{-5}	0.6349×10^{-6}
4	0	-0.8989×10^{-5}	...
	1	0.8125×10^{-5}	0.1862×10^{-5}
	2	-0.2822×10^{-5}	-0.1717×10^{-5}
	3	-0.1828×10^{-6}	-0.1571×10^{-5}
	4	0.6060×10^{-7}	-0.2726×10^{-6}
5	0	0.3220×10^{-5}	...
	1	-0.3245×10^{-5}	-0.1005×10^{-4}
	2	0.8523×10^{-6}	-0.6792×10^{-6}
	3	-0.4586×10^{-6}	0.8224×10^{-6}
	4	-0.2826×10^{-7}	0.1271×10^{-7}
	5	-0.1936×10^{-9}	0.3457×10^{-9}
6	0	0.1506×10^{-4}	...
	1	0.1551×10^{-4}	-0.5958×10^{-5}
	2	-0.1652×10^{-5}	-0.6825×10^{-6}
	3	-0.2460×10^{-6}	-0.1144×10^{-6}
	4	-0.5457×10^{-7}	-0.1924×10^{-7}
	5	0.2515×10^{-8}	-0.2040×10^{-7}
	6	-0.3282×10^{-10}	-0.9527×10^{-9}
7	0	0.5640×10^{-4}	...
	1	0.5677×10^{-5}	-0.7902×10^{-5}
	2	-0.5746×10^{-6}	-0.1048×10^{-5}
	3	-0.6442×10^{-7}	0.3588×10^{-7}
	4	-0.1880×10^{-7}	0.6937×10^{-8}
	5	-0.5815×10^{-9}	0.4537×10^{-8}
	6	-0.5716×10^{-9}	0.8406×10^{-9}
	7	-0.1045×10^{-9}	0.1266×10^{-9}

the prediction capability of a gravity field is improved as the degree and order of the solution set is extended.

Residual Characteristics

The phenomenon of residual oscillations at periapse is shown in Fig. 3. The results in this figure are typical of those obtained in the solution for harmonic coefficients through degree and order 7. The source of the terminology used to describe these residuals is evident from the upper plot, which shows a high-frequency, high-amplitude oscillation in the vicinity of periapse passage, in this case, for the Lunar Orbiter V vehicle. This oscillation is quickly damped as the spacecraft moves from the low altitude at periapse to the high altitude at apoapse (100 km and 1500 km, respectively, for this case). This altitude damping effect is consistent with the philosophy that the source of these residuals is the

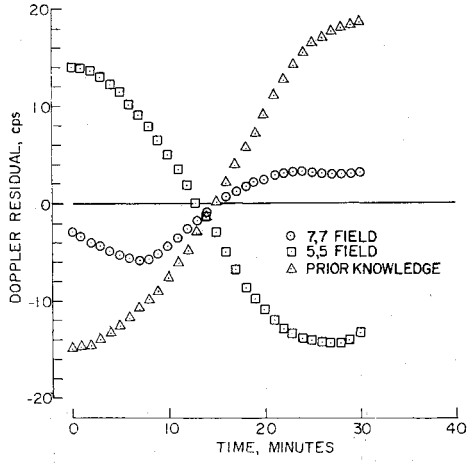

Fig. 2 Comparison of the predicted properties of various gravity fields for Lunar Orbiter IIIb.

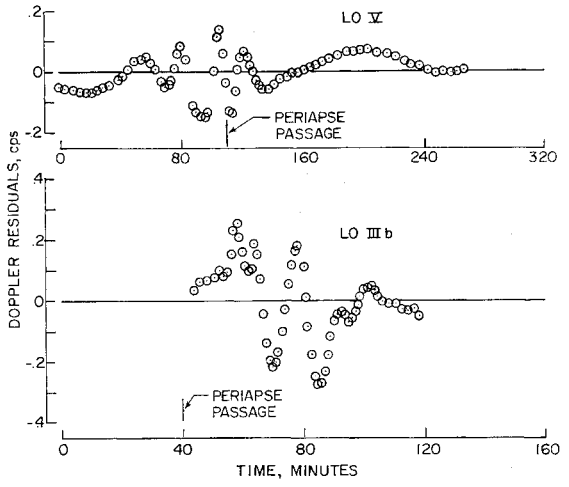

Fig. 3 Typical Doppler residuals for Lunar Orbiters V and IIIb.

gravitational field of the moon and that their existence indicates an incomplete mathematical representation of this field. This line of reasoning is supported by the lower plot which shows residuals spanning one orbit of the nearly circular phase of Lunar Orbiter III. The altitude variation over this orbit is from 120 to 340 km and the residual oscillations are distributed throughout the orbit.

The problem of residual oscillations has been receiving considerable attention at various research centers. The procedure at Langley Research Center has been one of attempting to absorb these residuals into the mathematical description of the lunar gravitational field by extending the degree and order of the terms used in this description. At the present time, the solution is being extended to coefficients of degree and order 11.

The effect of an increase in the number of coefficients in the solution set is shown in Fig. 4, where representative residuals from the low-eccentricity orbit of Lunar Orbiter III are presented for gravity fields of degree and order 4, 7, and 11. As the size of the solution set is increased, there is a reduction in the amplitude and an increase in the frequency of the residual oscillations. This is exactly the effect that would be expected if, as assumed, the residual oscillations are due to higher-order gravity terms not accounted for by the solution. For the degree and order 11 field, the small oscillations evident in the figure are not centered about the axis since the solution is not yet converged. It is to be noted from the residual characteristics in this case that even higher-order

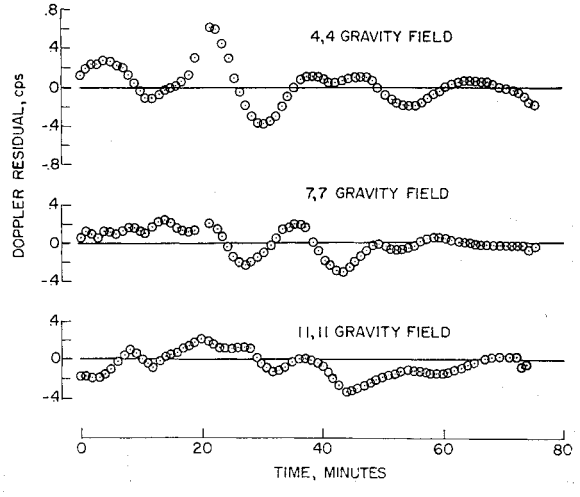

Fig. 4 Variation of Lunar Orbiter III residuals with degree and order of the coefficient solution set.

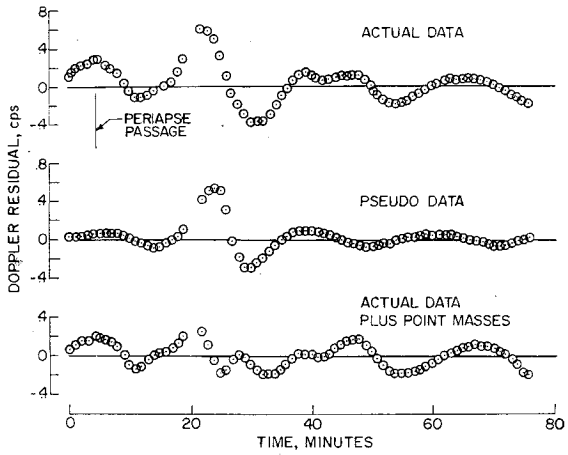

Fig. 5 Effect of point masses on the residual characteristics for a fourth degree and order fit to Lunar Orbiter IIIb data.

terms will have to be included in the solution before the residuals fall within the noise level of the data.

One interesting feature of the residual characteristics which has been noted from the data from the low-eccentricity orbit of Lunar Orbiter III is that the maximum amplitude of the residual oscillations does not always occur at satellite periapse position. One implication of this phenomenon is that lunar surface anomalies may be affecting the satellite orbit. This implication is somewhat disturbing since the representation of such effects would involve the necessity of including very high degree and order terms in the solution.

The results of a preliminary analysis of this phenomenon are shown in Fig. 5. The residuals which result from a 4th degree and order representation of the gravity field are shown on the first data plot. The large amplitude residuals in this case do not occur at the time of periapse passage. The 2nd data plot represents a fourth degree and order fit to pseudo-observational data generated for a gravitational model consisting of the central term, the C_{20} term, and three point masses (of the order of 10^{17} kg) distributed along the surface track of the satellite. The similarity of these two residual plots indicates that local surface anomalies can produce a residual pattern similar to the real data. The lower plot in this figure shows the residuals which remain from a solution utilizing the real tracking data with a 4th degree and order field and the same point masses. The residual pattern has changed considerably, and the change is similar in nature to that shown in Fig. 4 where the solution set was increased from a 4th to a 7th degree and order field. Although this analysis is very preliminary in nature, it is apparent that surface mass anomalies will have to be taken into account either by an extension of the solution set or by the inclusion of point masses directly in the solution.

The subject of lunar mass anomalies has been illustrated very graphically by Muller and Sjogren in Ref. 9, where the results of an analysis of the tracking data indicate large mass concentrations under the lunar ringed maria. Apart from the scientific importance of their findings, the results may be used as an additional test of the validity of a specified set of gravitational coefficients. If the assumption is made of a uniform density distribution, contours of the topography of the moon can be derived from the gravitational coefficients, and these contours may then be interpreted as local deviations in the mass of the moon. Based on this type of analysis, the lunar ringed maria would be represented by regions of positive elevations.

Application of such a technique to the coefficients presented in Table 2 was not wholly satisfactory; a result which was not unexpected in view of the conclusions of the previous paragraphs with relation to the necessity of increasing the size of the solution set. Application of this technique was

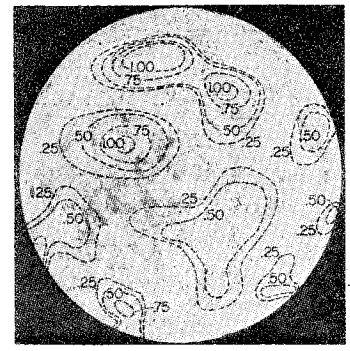

Fig. 6 Surface contours derived from gravitational coefficients; deviations in km from mean radius of 1738 km.

also made to the degree and order 11 field mentioned previously, and the results are shown in Fig. 6. These results should be interpreted with caution, since the coefficients do not represent a converged solution. However, the results do show considerable similarity with the results of Ref. 9, particularly in the regions of Mare Imbrium, Serenitatius, and Crisuim. Differences do exist, notably in the region of the crater Copernicus, which is indicated in Fig. 6 as a region of concentrated mass. However, until the results from a final solution are obtained and analyzed together with the results from contemplated increases in the solution set, no inference can be drawn from these differences. It is apparent, however, that the solution for the lunar gravitational field must include coefficients of at least degree and order 11.

Concluding Remarks

The results presented in this paper have indicated that an accurate representation of the lunar gravitational field requires the inclusion of coefficients of very high degree and order. At the present time, the results are being extended to include terms of degree and order 11. However, the residual characteristics indicate that even further extensions are required. This appears to be particularly true if the results are to be utilized for orbit prediction for satellites with low eccentricity, nearly circular orbits.

References

[1] Tolson, R. H. and Gapcynski, J. P., "An Analysis of the Lunar Gravitational Field as Obtained from Lunar Orbiter Tracking Data," paper presented at IQSY/COSPAR Assemblies, London, England, July 17–28, 1967.

[2] Michael, W. H., Jr., "Physical Properties of the Moon as Obtained from Lunar Orbiter Data," presented at the 14th General Assembly of the International Union of Geodesy and Geophysics Meeting, Lucerne, Switzerland, Sept. 1967.

[3] Blackshear, W. T., Compton, H. R., and Schiess, J. R., "Preliminary Results on the Lunar Gravitational Field from Analysis of Long-Period and Secular Effects on Lunar Orbiter I," presented at NASA Seminar on Guidance Theory and Trajectory Analysis, Electronics Research Center, Cambridge, Mass., May 1967.

[4] Lorell, J. and Sjogren, W. L., "Lunar Gravity: Preliminary Estimates from Lunar Orbiter," Vol. 159, No. 3815, Feb. 1968, p. 625.

[5] Mulholland, J. D. and Sjogren, W. L., "Lunar Orbiter Ranging Data: Initial Results," Vol. 155, Jan. 1967, p. 74.

[6] Michael, W. H., Jr., Tolson, R. H., and Gapcynski, J. P., "Preliminary Results on the Gravitational Field of the Moon from Analysis of Lunar Orbiter Tracking Data," paper presented at the American Geophysical Union Annual Meeting, Washington, D. C., April 17–20, 1967.

[7] Michael, W. H., Jr., Tolson, R. H., and Gapcynski, J. P., "Lunar Orbiter: Tracking Data Indicate Properties of Moon's Gravitational Field," *Science*, Vol. 153, No. 3740, Sept. 2, 1966, pp. 1102–1103.

[8] Lorell, J. and Sjogren, W. L., "Lunar Orbiter Data Analysis," TR 32-1220, Nov. 1967, Jet Propulsion Lab., California Institute of Technology.

[9] Muller, P. M. and Sjogren, W. L., "Mascons: Lunar Mass Concentrations," *Science*, Vol. 161, No. 3842, Aug. 16, 1968, pp. 680–684.